

# Probing the Influence of Stereoelectronic Effects on the Biophysical Properties of Oligonucleotides: Comprehensive Analysis of the RNA Affinity, Nuclease Resistance, and Crystal Structure of Ten 2'-O-Ribonucleic Acid Modifications<sup>†,‡</sup>

Martin Egli,<sup>\*,§</sup> George Minasov,<sup>||</sup> Valentina Tereshko,<sup>⊥</sup> Pradeep S. Pallan,<sup>§</sup> Marianna Teplova,<sup>#</sup> Gopal B. Inamati,<sup>∇</sup> Elena A. Lesnik,<sup>∇</sup> Steve R. Owens,<sup>∇</sup> Bruce S. Ross,<sup>∇</sup> Thazha P. Prakash,<sup>∇</sup> and Muthiah Manoharan<sup>\*,○</sup>

Department of Biochemistry, Vanderbilt University, Nashville, Tennessee 37232, Department of Molecular Pharmacology and Biological Chemistry, Northwestern University, Chicago, Illinois 60611, Department of Biochemistry and Molecular Biology, University of Chicago, Illinois 60637, Department of Molecular Biology and Biophysics, Memorial Sloan-Kettering Cancer Center, New York, New York 10021, Department of Medicinal Chemistry, Isis Pharmaceutical Inc., Carlsbad, California 92008, and Department of Drug Discovery, Alnylam Pharmaceuticals Inc., Cambridge, Massachusetts 02142

Received March 29, 2005; Revised Manuscript Received May 5, 2005

**ABSTRACT:** The syntheses of 10 new RNA 2'-O-modifications, their incorporation into oligonucleotides, and an evaluation of their properties such as RNA affinity and nuclease resistance relevant to antisense activity are presented. All modifications combined with the natural phosphate backbone lead to significant gains in terms of the stability of hybridization to RNA relative to the first-generation DNA phosphorothioates (PS-DNA). The nuclease resistance afforded in particular by the 2'-O-modifications carrying a positive charge surpasses that of PS-DNA. However, small electronegative 2'-O-substituents, while enhancing the RNA affinity, do not sufficiently protect against degradation by nucleases. Similarly, oligonucleotides containing 3'-terminal residues modified with the relatively large 2'-O-[2-(benzyloxy)ethyl] substituent are rapidly degraded by exonucleases, proving wrong the assumption that steric bulk will generally improve protection against nuclease digestion. To analyze the factors that contribute to the enhanced RNA affinity and nuclease resistance we determined crystal structures of self-complementary A-form DNA decamer duplexes containing single 2'-O-modified thymidines per strand. Conformational preorganization of substituents, favorable electrostatic interactions between substituent and sugar–phosphate backbone, and a stable water structure in the vicinity of the 2'-O-modification all appear to contribute to the improved RNA affinity. Close association of positively charged substituents and phosphate groups was observed in the structures with modifications that protect most effectively against nucleases. The promising properties exhibited by some of the analyzed 2'-O-modifications may warrant a more detailed evaluation of their potential for in vivo antisense applications. Chemical modification of RNA can also be expected to significantly improve the efficacy of small interfering RNAs (siRNA). Therefore, the 2'-O-modifications introduced here may benefit the development of RNAi therapeutics.

The search for nucleic acid analogues with optimal properties for potential applications as antisense therapeutics

has prompted the synthesis and biochemical characterization of hundreds of modifications over the past decade (1). The first-generation phosphorothioate oligodeoxynucleotides (PS-DNA) offer a number of advantages, such as ease of synthesis, nuclease resistance sufficient for parenteral administration, activation of RNase H for clearing the target RNA, and sufficiently large binding to cellular and serum proteins for uptake, absorption, and distribution (2). However, PS-DNAs also revealed limitations with regard to their use as antisense therapeutics because of their relatively low binding affinity to RNA (ca. 1 °C < DNA per modified nucleotide), the inhibition of RNase H at high concentration, and their nonspecific binding to proteins. Moreover, PS-DNAs do not penetrate the blood–brain barrier and they show poor oral bioavailability (3).

Among the potential sites for chemical modification available in DNA the 2'-position is particularly attractive. Substitution of the 2'-hydrogen in the ribo configuration with an electronegative moiety locks the pentofuranose in a C3'-endo conformation (the structure preferred by the RNA target strand) due to the gauche effect between O4' and the 2'-

<sup>†</sup> Supported by NIH Grant GM55237 (M.E.). Use of the Advanced Photon Source was supported by the U.S. Department of Energy, Basic Energy Sciences, Office of Science, under Contract No. W-31-109-Eng-38. The DuPont-Northwestern-Dow Collaborative Access Team (DND-CAT) Synchrotron Research Center at the Advanced Photon Source (Sector 5) is supported by E. I. DuPont de Nemours & Co., The Dow Chemical Company, the National Science Foundation, and the State of Illinois.

<sup>‡</sup> Coordinates and structure factors for all structures have been deposited in the Protein Data Bank (<http://www.rcsb.org>). The accession codes are 1Y8V (PRL), 1WV5 (BTL-Mg), 1WV6 (BTL-Sr), 1Y86 (FET), 1Y8L (TFE), 1Y9F (ALY), 1Y9S (PRG), 1YBC (BOE), 1Y9B (DMAOE), 1Y7F (MAOE), and 1Y84 (IME).

\* Corresponding authors. M.E.: phone, +1 (615) 343-8070; fax, +1 (615) 322-7122; e-mail, [martin.egli@vanderbilt.edu](mailto:martin.egli@vanderbilt.edu). M.M.: phone, +1 (617) 551-8319; fax, +1 (617) 551-8102; e-mail, [mmanoharan@alnylam.com](mailto:mmanoharan@alnylam.com).

<sup>§</sup> Vanderbilt University.

<sup>||</sup> Northwestern University.

<sup>⊥</sup> University of Chicago.

<sup>#</sup> Memorial Sloan-Kettering Institute.

<sup>∇</sup> Isis Pharmaceuticals.

<sup>○</sup> Alnylam Pharmaceuticals.

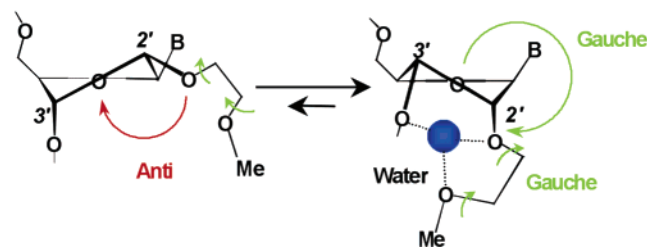
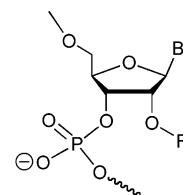


FIGURE 1: Gauche effects in 2'-O-MOE RNA that drive the sugar conformational equilibrium toward the C3'-endo pucker.

substituents (Figure 1) (4). Modification with 2'-O-alkyl substituents improves RNA affinity and leads to enhanced nuclease resistance (5, 6). The latter is directly correlated with the length of the alkyl chain, whereas the correlation between substituent length and RNA affinity is inverse. The relatively short 2'-O-[2-(methoxy)ethyl] modification (MOE) confers increased RNA affinity ( $\Delta T_m$  ca. 2 °C/modification relative to PS-DNA) and nuclease resistance (similar to PS-DNA) (7–10). Using an in situ single-pass rat intestinal perfusion model, 2'-O-modified oligonucleotides exhibited 2.5- to 10-fold increased permeability (11). X-ray crystal structures of an all-modified 2'-O-MOE modified dodecamer duplex and A-form DNA decamer duplex carrying single 2'-O-MOE modifications per strand pointed to conformational preorganization and substituent hydration as potential reasons for the higher stability of 2'-O-MOE-RNA:RNA compared to PS-DNA:RNA duplexes (12, 13). Moreover, the lower toxicity of 2'-O-MOE RNA relative to PS-DNA may be a consequence of the lower affinity of the former modification for serum proteins, in part due to the extensive hydration of the 2'-substituent.

Another ribose modification, 2'-O-(3-aminopropyl) (2'-O-AP) RNA, shows superb nuclease resistance even in combination with a phosphodiester (PO) backbone (14). A crystallographic analysis of 2'-O-AP-modified oligonucleotides bound at the active site of an exonuclease revealed displacement of a catalytically important metal cation by the positively charged aminopropyl substituent (15). The 2'-O-[2-[2-(*N,N*-dimethylamino)ethoxy]ethyl] (2'-O-DMAEOE) modification merges the high RNA affinity of the 2'-O-MOE with the superior nuclease resistance of the 2'-O-AP modification (16). A further analogue, the sulfur equivalent of 2'-O-MOE, the 2'-O-[2-(methylthio)ethyl] (2'-O-MTE) modification, was found to exhibit improved binding to serum proteins but had relatively limited resistance to degradation by nucleases (17).

In order to potentially identify further 2'-O-modified nucleic acid analogues with interesting properties for anti-sense applications and to better understand the relation between RNA affinity and nuclease resistance of an analogue and the conformation and hydration of the 2'-substituent, we conducted a comprehensive analysis of 10 2'-O-modified analogues. Here, we report the chemical synthesis, RNA affinity, resistance to exonuclease degradation, and crystal structure of these modifications. The investigated 2'-O-substituents include short aliphatic (propyl, butyl), electro-negative (fluoro- and trifluoroethyl, allyl, propargyl), bulky (methyleneaminoxyethyl), aromatic (benzylloxyethyl), and charged (dimethylaminoxyethyl, imidazolylethyl) moieties<sup>1</sup> (Figure 2). The crystallographic analyses at high resolution (<1.8 Å except for one structure) demonstrate that confor-



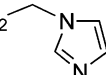
A: 2'-O-MOE:	R = CH <sub>2</sub> -CH <sub>2</sub> -O-CH <sub>3</sub>
B: 2'-O-PRL:	R = CH <sub>2</sub> -CH <sub>2</sub> -CH <sub>3</sub>
C: 2'-O-BTL:	R = CH <sub>2</sub> -CH <sub>2</sub> -CH <sub>2</sub> -CH <sub>3</sub>
D: 2'-O-FET:	R = CH <sub>2</sub> -CH <sub>2</sub> -F
E: 2'-O-TFE:	R = CH <sub>2</sub> -CF <sub>3</sub>
F: 2'-O-ALY:	R = CH <sub>2</sub> -CH=CH <sub>2</sub>
G: 2'-O-PRG:	R = CH <sub>2</sub> -C≡CH
H: 2'-O-BOE:	R = CH <sub>2</sub> -CH <sub>2</sub> -O-CH <sub>2</sub> -C <sub>6</sub> H <sub>5</sub>
I: 2'-O-DMAOE:	R = CH <sub>2</sub> -CH <sub>2</sub> -O-N(CH <sub>3</sub> ) <sub>2</sub>
J: 2'-O-MAOE:	R = CH <sub>2</sub> -CH <sub>2</sub> -O-N=CH <sub>2</sub>
K: 2'-O-IME:	R = CH <sub>2</sub> - 

FIGURE 2: Structure of the 2'-O-modifications.

mational preorganization (“gauche effect”), hydration, and electronegativity of the substituent are the major determinants of the increased RNA affinity of the 2'-O-modifications relative to both DNA and RNA. By comparison, charge effects and hydration but not necessarily bulkiness of the substituent appear to be chiefly at the origin of the high nuclease resistance of certain 2'-O-modified analogues that exceed that of PS-DNA in some instances.

## MATERIALS AND METHODS

**2'-O-(2-Methoxyethyl)-5-methyluridine (2).** Borane in tetrahydrofuran (1.0 M, 1.5 equiv, 30 mL) was added to a 100 mL unstirred pressure reactor. 2-Methoxyethanol (25 mL) was added cautiously to allow the evolution of hydrogen gas in a controlled manner. 2,2'-Anhydro-5-methyluridine **1** (5.0 g, 20 mmol) and sodium bicarbonate (10 mg) were added with manual stirring. The reaction mixture was added into a stainless steel pressure reactor and sealed. The sealed pressure reactor was placed in an oil bath at 150 °C (pressure <100 psig) for 16 h. The steel bomb was cooled to ambient temperature, opened, and assayed, and the reaction was found to be complete. The excess 2-methoxyethanol was removed under reduced pressure, and the residue was coevaporated with methanol (3 × 30 mL). The residue was triturated with ether (100 mL) to form a gum. After stirring overnight, the gum broke up into a solid. The solid was collected by filtration, washed with ether (20 mL), and dried. The crude

<sup>1</sup> Abbreviations: MOE, 2'-O-[2-(methoxy)ethyl]; PRL, 2'-O-propyl; BTL, 2'-O-butyl; FET, 2'-O-[2-(fluoro)ethyl]; TFE, 2'-O-[2-(trifluoro)ethyl]; ALY, 2'-O-allyl; PRG, 2'-O-propargyl; BOE, 2'-O-[2-(benzylloxy)ethyl]; DMAOE, 2'-O-[2-(*N,N*-dimethylaminoxy)ethyl]; MAOE, 2'-O-[2-[(methyleneamino)oxy]ethyl]; IME, 2'-O-[2-(imidazolyl)ethyl]; HAS, human serum albumin; PO, phosphodiester; PS, phosphorothioate; DMF, *N,N*-dimethylformamide; MeOH, methanol; EtOH, ethanol; DMTCl, 4,4'-dimethoxytrityl chloride; TLC, thin-layer chromatography; SVPD, snake venom phosphodiesterase; HRMS, high-resolution mass spectrum; DMAP, 4-(dimethylamino)pyridine; LCAA-CPG, long chain alkylamine controlled pore glass; TEAAc, triethylammonium acetate; HPLC, high performance liquid chromatography; CGE, capillary gel electrophoresis; Tris-HCl, tris(hydroxymethyl)aminoethane hydrochloride; TEA, triethylamine; MPD, 2-methyl-2,4-pentandiol.

product was purified by flash silica gel column chromatography and eluted with CH<sub>2</sub>Cl<sub>2</sub> containing incremental amount (5% to 10%) of methanol to yield **2** (3.95 g, 60% yield) as a white, hygroscopic solid. <sup>1</sup>H NMR (DMSO-*d*<sub>6</sub>): δ 1.75 (s, 3 H), 3.20 (s, 3H), 3.42 (t, *J* = 4.8 Hz, 2H), 3.54–3.64 (m, 4 H), 3.82 (m, 1H), 3.93 (t, *J* = 5.4 and 5 Hz, 1H), 4.09 (m, 1H), 5.00 (d, *J* = 5.6 Hz, 1H), 5.14 (t, *J* = 5 Hz, 1H), 5.83 (d, *J* = 5.2 Hz, 1 H), 7.76 (s, 1 H), 11.31 (s, 1 H). MS (AP-ES): *m/z* calculated for C<sub>13</sub>H<sub>21</sub>N<sub>3</sub>O<sub>7</sub> 317.3, found 317.1 [M + H]<sup>+</sup>.

**2'-O-(*n*-Butyl)-5-methyluridine (3)**. Compound **3** (7.59 g, 58% yield) was synthesized from borane in tetrahydrofuran (1.0 M, 83 mL), *n*-butanol (54 g, 728 mmol), 2,2'-anhydro-5-methyluridine **1** (10.0 g, 41.65 mmol), and sodium bicarbonate (80 mg) at 160 °C in a 2 L unstirred bomb for 18 h using a procedure similar to that used for the synthesis of **2**. MS (AP-ES): *m/z* calculated for C<sub>14</sub>H<sub>23</sub>N<sub>2</sub>O<sub>6</sub> 315.3, found 315.4 [M + H]<sup>+</sup>.

**2'-O-(2-Fluoroethyl)-5-methyluridine (4)**. Borane in tetrahydrofuran (1.0 M, 1.5 equiv, 30 mL) was added to a 100 mL unstirred pressure reactor. 2-Fluoroethanol (25 mL) was added cautiously to allow the evolution of hydrogen gas in a controlled manner. 2,2'-Anhydro-5-methyluridine **1** (5.0 g, 20 mmol) and sodium bicarbonate (10 mg) were added with manual stirring. The reaction mixture was transferred into a steel bomb sealed and placed in an oil bath at 150 °C (pressure <100 psig) for 16 h. The vessel was cooled to ambient temperature, opened, and assayed, and the reaction was found to be complete. The excess 2-fluoroethanol was removed under reduced pressure, and the residue was coevaporated with methanol (3 × 30 mL). The residue was triturated with ether (100 mL) to form a gum. After stirring overnight, the gum broke up into a solid. The solid was collected by filtration, washed with ether (20 mL), and dried to yield **4** (4.11 g, 65%) as a white, hygroscopic solid. The crude product obtained was used for the next step without purification. MS (AP-ES): *m/z* calculated for C<sub>12</sub>H<sub>18</sub>FN<sub>2</sub>O<sub>6</sub> 305.2, found 305.3 [M + H]<sup>+</sup>.

**2'-O-(2-Trifluoroethyl)-5-methyluridine (5)**. Compound **5** (12.1 g, 28%) was synthesized from 2,2'-anhydro-5-methyluridine **1** (30.0 g, 0.12 mol) using a procedure similar to that used for the synthesis of **4**. Borane in tetrahydrofuran (1.0 M, 2.0 equiv, 250 mL), 2-(trifluoro)ethanol (150 mL), and sodium bicarbonate (40 mg) were also used at 160 °C in a 2 L unstirred steel bomb for 18 h. One-third of the starting 2,2'-anhydro-5-methyluridine material remained unreacted. The excess 2-(trifluoro)ethanol was removed under reduced pressure, and the residue obtained was dissolved in a minimum amount of ethyl acetate–methanol (8:2), loaded onto a flash silica gel column chromatography, and eluted with ethyl acetate. <sup>1</sup>H NMR (DMSO-*d*<sub>6</sub>): δ 1.578 (s, 3 H), 3.50–4.20 (m, 9 H), 4.10–4.25 (m, 2 H), 5.83 (d, *J* = 5.62 Hz, 1 H), 7.81 (s, 1 H), 11.35 (s, 1 H). <sup>19</sup>F NMR (DMSO-*d*<sub>6</sub>): δ 74.5 (s). MS (AP-ES): *m/z* calculated for C<sub>12</sub>H<sub>16</sub>F<sub>3</sub>N<sub>2</sub>O<sub>6</sub> 341.2, found 341.24 [M + H]<sup>+</sup>.

**2'-O-Allyl-5-methyluridine (6)**. In a 1 L stainless steel pressure reactor, allyl alcohol (200 mL) was slowly added to a solution of borane in tetrahydrofuran (1 M, 100 mL, 100 mmol) with stirring. Hydrogen gas rapidly evolved. Once the rate of bubbling subsided, 2,2'-anhydro-5-methyluridine (10.00 g, 41.63 mmol) and sodium bicarbonate (60 mg) were added and the bomb was sealed. The reactor was placed in

an oil bath and heated at 170 °C internal temperature for 18 h. The bomb was cooled to room temperature and opened. The solvent was removed under reduced pressure to yield an oil. The oil thus obtained was coevaporated with methanol (50 mL), boiling water (15 mL), and absolute ethanol (2 × 25 mL). The residue obtained was purified by flash silica gel column chromatography and eluted with 5–10% methanol in dichloromethane to yield **6** (6.84 g, 55%). MS (AP-ES): *m/z* calculated for C<sub>13</sub>H<sub>19</sub>N<sub>2</sub>O<sub>6</sub> 299.1, found 299.3 [M + H]<sup>+</sup>.

**2'-O-Propargyl-5-methyluridine (7)**. Compound **7** (14.4 g, 41% yield, white foam) was synthesized from borane in tetrahydrofuran (1.0 M, 2.0 equiv, 250 mL), propargyl alcohol (200 mL), 2,2'-anhydro-5-methyluridine (30.0 g, 120 mmol), and sodium bicarbonate (40 mg) in an oil bath at 160 °C in a stainless steel pressure reactor for 18 h using a procedure similar to that used for **4**. The residue obtained after workup was dissolved in methanol, adsorbed on silica gel, loaded onto a flash silica gel column, and eluted with a gradient of methanol in ethyl acetate (0–10%). <sup>1</sup>H NMR (DMSO-*d*<sub>6</sub>): δ 1.79 (s, 3 H), 2.5 (m, 1 H), 3.60 (m, 2 H), 3.83 (m, 1 H), 4.05–4.30 (m, 4 H), 5.20 (m, 2 H), 5.84 (d, *J* = 5.91 Hz, 1 H), 7.78 (s, 1 H), 11.37 (s, 1 H). MS (AP-ES): *m/z* calculated for C<sub>13</sub>H<sub>17</sub>N<sub>2</sub>O<sub>6</sub> 297.1, found 297.2 [M + H]<sup>+</sup>.

**2'-O-(2-Benzoyloxyethyl)-5-methyluridine (8)**. Compound **8** (4.50 g, 55% yield) was synthesized from borane in tetrahydrofuran (1.0 M, 2.0 equiv, 42 mL), 2-(benzyloxy)ethanol (25 mL), 2,2'-anhydro-5-methyluridine **1** (5.0 g, 21.00 mmol), and sodium bicarbonate (10 mg) using a procedure similar to that described for compound **4**. <sup>1</sup>H NMR (DMSO-*d*<sub>6</sub>): δ 1.75 (s, 3 H), 3.40–3.78 (m, 6 H), 3.83 (m, 1 H), 4.02 (m, 1 H), 4.13 (m, 1 H), 4.45 (s, 2 H), 5.05 (d, *J* = 5.23 Hz, 1 H), 5.16 (t, *J* = 5.61 Hz, 1 H), 5.85 (d, *J* = 6.12 Hz, 1 H), 7.20–7.40 (m, 6 H), 11.38 (s, 1 H). MS (AP-ES): *m/z* calculated for C<sub>19</sub>H<sub>25</sub>N<sub>2</sub>O<sub>7</sub> 393.4, found 393.6 [M + H]<sup>+</sup>.

**2'-O-(2-(Imidazol-1-yl)ethyl)-5-methyluridine (9)**. Compound **9** (2.48 g, 35% yield) was synthesized from borane in tetrahydrofuran (1.0 M, 2.0 equiv, 42 mL), 2-(imidazol-1-yl)ethanol (20 g, 178.48 mmol), 2,2'-anhydro-5-methyluridine (5.0 g, 21.00 mmol), and sodium bicarbonate (10 mg) using a procedure similar to that described for compound **4**. MS (AP-ES): *m/z* calculated for C<sub>15</sub>H<sub>21</sub>N<sub>4</sub>O<sub>6</sub> 353.3, found 353.4 [M + H]<sup>+</sup>.

**5'-O-(4,4'-Dimethoxytrityl)-2'-O-(2-methoxyethyl)-5-methyluridine (10)**. Compound **2** (3.5 g, 11.07 mmol) was coevaporated with pyridine (2 × 20 mL), and the residue obtained was dissolved in anhydrous pyridine (50 mL). 4,4'-Dimethoxytrityl chloride (4.88 g, 14.39 mmol) was added in one portion, and the solution was stirred at ambient temperature under argon for 6 h. The reaction was quenched with methanol (2 mL), and solvent was removed under reduced pressure. The residue was partitioned between ethyl acetate (200 mL) and saturated aqueous sodium bicarbonate (100 mL). The organic phase was separated and evaporated under reduced pressure to yield an oil. The oil was then purified by flash silica gel column chromatography and eluted with ethyl acetate/hexane/triethylamine, 79:20:1, to yield **10** (5.48 g, 80% yield) as a white foam. <sup>1</sup>H NMR (DMSO-*d*<sub>6</sub>): δ 1.38 (s, 3 H), 3.22 (s, 3H), 3.43 (m, 1H), 3.46 (t, *J* = 4.8 Hz, 2H), 3.54–3.64 (m, 4 H), 3.82 (m, 1H), 3.93 (t, *J* = 5.4 and 5 Hz, 1H), 4.09 (m, 1H), 5.00 (d, *J* =

5.6 Hz, 1H), 5.14 (t,  $J = 5$  Hz, 1H), 5.83 (d,  $J = 5.2$  Hz, 1H), 7.76 (s, 1H), 11.31 (s, 1H). MS (AP-ES):  $m/z$  calculated for  $C_{34}H_{38}N_2NaO_9$  641.7, found 641.9 [M + Na]<sup>+</sup>.

*5'-O-(4,4'-Dimethoxytrityl)-2'-O-(n-butyl)-5-methyluridine (11)*. Compound **11** (11.67 g, 85% yield) was synthesized from **3** (7.00 g, 22.27 mmol), 4,4'-dimethoxytrityl chloride (9.05 g, 26.72 mmol), and 150 mL of anhydrous pyridine with stirring of the reaction mixture for 8 h using a procedure similar to that used for the synthesis of **14**. MS (AP-ES):  $m/z$  calculated for  $C_{35}H_{40}N_2NaO_8$  639.7, found 639.6 [M + Na]<sup>+</sup>.

*5'-O-(4,4'-Dimethoxytrityl)-2'-O-(2-fluoroethyl)-5-methyluridine (12)*. Compound **4** (5 g, 16.43 mmol) was coevaporated with pyridine (2 × 20 mL), and the residue obtained was dissolved in anhydrous pyridine (40 mL). 4,4'-Dimethoxytrityl chloride (7.0 g, 20.66 mmol) was added in one portion, and the solution was stirred at ambient temperature under argon for 1 h. The reaction was quenched with methanol (5 mL), and solvent was removed under reduced pressure. The residue was partitioned between ethyl acetate (200 mL) and saturated aqueous sodium bicarbonate (100 mL). The organic phase was separated and evaporated under reduced pressure to yield an oil. The oil was then purified by flash silica gel column chromatography and eluted with ethyl acetate/hexane/triethylamine, 79:20:1, to yield **12** (4.9 g, 49%) as a white foam. <sup>1</sup>H NMR (200 MHz, DMSO-*d*<sub>6</sub>):  $\delta$  1.42 (s, 3 H), 3.20–3.40 (m, 2 H), 3.79 (s, 6 H), 3.90–4.08 (m, 3H), 4.14 (m, 2 H), 4.26 (m, 1 H), 4.59 (d,  $J = 48$  Hz, 2 H), 5.28 (d,  $J = 5.2$  Hz, 1 H), 5.88 (d,  $J = 6.1$  Hz, 1 H), 6.93 (d,  $J = 8.63$  Hz, 4H), 7.20–7.45 (m, 9 H), 7.53 (s, 1 H), 11.43 (s, 1 H). MS: (AP-ES):  $m/z$  calculated for  $C_{33}H_{36}FN_2O_8$  607.6, found 607.8 [M + H]<sup>+</sup>.

*5'-O-(4,4'-Dimethoxytrityl)-2'-O-(2-trifluoroethyl)-5-methyluridine (13)*. Compound **5** (14.56 g, 42.81 mmol) was coevaporated with pyridine (2 × 100 mL), and the residue obtained was dissolved in anhydrous pyridine (100 mL). 4,4'-Dimethoxytrityl chloride (DMTCl, 15.96 g, 47.10 mmol) was added, and the reaction mixture was stirred under argon at room temperature for 16 h. TLC indicated an incomplete reaction. An additional 10 g of DMTCl was added and stirring continued for an additional 1 h. The reaction was quenched with methanol (25 mL), and solvent was removed under reduced pressure. The residue was partitioned between ethyl acetate (500 mL) and saturated aqueous sodium bicarbonate (300 mL). The organic phase was separated and concentrated under reduced pressure to yield an oil. The oil was then purified by flash silica gel column chromatography and eluted first with ethyl acetate/hexane/triethylamine (79:20:1) and then with 5% of MeOH in CH<sub>2</sub>Cl<sub>2</sub> to yield **13** (17.56 g, 61%). <sup>1</sup>H NMR (200 MHz, DMSO-*d*<sub>6</sub>):  $\delta$  1.41 (s, 3 H), 3.20–3.35 (m, 2 H), 3.75 (s, 6 H), 3.95 (m, 1 H), 3.95–4.12 (m, 2 H), 4.20–4.41 (m, 3 H), 5.48 (d,  $J = 5.62$  Hz, 1 H), 5.87 (d,  $J = 6.3$  Hz, 1 H), 6.85 (d,  $J = 8.6$  Hz, 4H), 7.20–7.43 (m, 9 H), 7.52 (s, 1 H), 11.43 (s, 1 H).

*5'-O-(4,4'-Dimethoxytrityl)-2'-O-allyl-5-methyluridine (14)*. Compound **6** (1.2 g, 4.02 mmol) was coevaporated with anhydrous pyridine (30 mL). The residue obtained was dissolved in anhydrous pyridine (30 mL). 4,4'-Dimethoxytrityl chloride (1.7 g, 5.0 mmol) was added, and the reaction mixture was stirred for 4 h. The reaction was quenched with methanol (5 mL), and solvent was removed under reduced pressure. The residue obtained was partitioned between

saturated sodium bicarbonate solution (50 mL) and ethyl acetate (50 mL). The organic phase was separated, dried over anhydrous Na<sub>2</sub>SO<sub>4</sub>, and concentrated under reduced pressure. The residue was purified by flash silica gel column chromatography and eluted with hexane/ethyl acetate/triethylamine (50:49:1 to 60:39:1) to yield **14** (0.84 g, 34%). <sup>1</sup>H NMR (DMSO-*d*<sub>6</sub>):  $\delta$  1.37 (s, 3 H), 3.22 (m, 2 H), 3.76 (s, 6 H), 3.95–4.35 (m, 5 H), 5.16–5.34 (m, 3 H), 5.82–6.03 (m, 2 H), 6.92 (d,  $J = 8.62$  Hz, 4H), 7.20–7.42 (m, 9H), 7.52 (s, 1 H), 11.42 (s, 1 H).

*5'-O-(4,4'-Dimethoxytrityl)-2'-O-propargyl-5-methyluridine (15)*. Compound **15** (18.0 g, 81% yield) was synthesized from **7** (11.4 g, 39.0 mmol), 4,4'-dimethoxytrityl chloride (15.62 g, 46.10 mmol), and 100 mL of anhydrous pyridine with stirring of the reaction mixture for 16 h using a procedure similar to that used for the synthesis of **14**. MS (AP-ES):  $m/z$  calculated for  $C_{34}H_{34}N_2NaO_8$  621.2, found 621.6 [M + Na]<sup>+</sup>.

*5'-O-(4,4'-Dimethoxytrityl)-2'-O-(2-benzyloxyethyl)-5-methyluridine (16)*. From compound **8** (2.8 g, 7.13 mmol), 4,4'-dimethoxytrityl chloride (2.9 g, 8.56 mmol), and 20 mL of pyridine and with stirring of the reaction mixture for 2.5 h, compound **16** (3.22 g, 65% yield) was synthesized using a procedure similar to that used for the synthesis of **14**. <sup>1</sup>H NMR (DMSO-*d*<sub>6</sub>):  $\delta$  1.40 (s, 3 H), 3.15–3.45 (m, 2 H), 3.60 (t,  $J = 5.36$  Hz, 2 H), 3.65–3.80 (m, 8 H), 3.95 (m, 1 H), 4.11 (m, 1 H), 4.24 (m, 1 H), 4.48 (s, 2 H), 5.17 (d,  $J = 5.43$  Hz, 1 H), 5.85 (d,  $J = 5.94$  Hz, 1 H), 6.86 (d,  $J = 8.62$  Hz, 4H), 7.20–7.43 (m, 14 H), 7.50 (s, 1 H), 11.42 (s, 1 H).

*5'-O-(4,4'-Dimethoxytrityl)-2'-O-(2-(imidazol-1-yl)ethyl)-5-methyluridine (17)*. From compound **9** (2.20 g, 6.46 mmol), 4,4'-dimethoxytrityl chloride (2.63 g, 7.75 mmol), and 45 mL of pyridine and with stirring for 4 h, compound **17** (2.53 g, 60% yield) was synthesized using the a procedure similar to that used for the synthesis of **14**. MS (AP-ES):  $m/z$  calculated for  $C_{36}H_{39}N_4O_8$  655.3, found 655.7 [M + H]<sup>+</sup>.

*Synthesis of 3'-Phosphoramidites 18–25*. The nucleosides **10–17** were coevaporated with anhydrous acetonitrile (3 × 10 mL g<sup>-1</sup>) and then dissolved in anhydrous dichloromethane (10 mL g<sup>-1</sup>). Diisopropylamino tetrazolide (0.3 molar equiv) was added followed by 2-cyanoethyl-*N,N,N',N'*-tetraisopropylphosphorodiamidite (1.2 molar equiv). The reaction mixture was stirred under an argon atmosphere until the reaction was completed as monitored by thin-layer chromatography (TLC). The reaction mixture was washed with saturated aqueous sodium bicarbonate (20 mL g<sup>-1</sup>) and brine (20 mL g<sup>-1</sup>) and the organic phase separated and dried over anhydrous sodium sulfate and concentrated to yield a foam. The foam was redissolved in a minimum amount of dichloromethane, loaded onto a flash silica gel column (10–20 g g<sup>-1</sup>), and eluted with ethyl acetate (40–100%) in hexanes containing 1% triethylamine. The fractions containing the products were pooled together, and solvent was removed under reduced pressure to yield phosphoramidites as foam.

*5'-O-(4,4'-Dimethoxytrityl)-2'-O-(2-methoxyethyl)-5-methyluridine-3'-[(2-cyanoethyl)-*N,N*-diisopropyl]phosphoramidite (18)*. Following the general synthetic procedure for phosphoramidite synthesis (vide supra), the nucleoside **10** (3.0 g, 4.85 mmol) was converted to **18** (3.30 g, 83% yield). <sup>31</sup>P NMR (80 MHz, CDCl<sub>3</sub>)  $\delta$  151.82, 151.13.

*5'-O-(4,4'-Dimethoxytrityl)-2'-O-(n-butyl)-5-methyluridine-3'-[(2-cyanoethyl)-*N,N*-diisopropyl]phosphoramidite (19)*.

Table 1: Effect of 2'-O-Modification on Duplex Stability against Complementary RNA Relative to DNA

entry	T*	L <sup>a</sup>		M <sup>b</sup>		N <sup>c</sup>	
		T <sub>m</sub> (°C) <sup>d</sup>	ΔT <sub>m</sub> per mod (°C)	T <sub>m</sub> (°C) <sup>d</sup>	ΔT <sub>m</sub> per mod (°C)	T <sub>m</sub> (°C) <sup>d</sup>	ΔT <sub>m</sub> per mod (°C)
	T	62.3		48.3		61.8	
A	2'-O-MOE- <sup>5</sup> MeU	65.8	0.9	65.3	0.9	59.8	1.2
B	2'-O-PRL- <sup>5</sup> MeU	65.1	0.7	64.4	0.7	55.9	0.8
C	2'-O-BTL- <sup>5</sup> MeU	64.6	0.6	64.1	0.6	56.6	0.8
D	2'-O-FET- <sup>5</sup> MeU	67.9	1.4	66.3	1.1	61.6	1.3
E	2'-O-TFE- <sup>5</sup> MeU	65.7	0.8	65.8	1.0	60.5	1.2
F	2'-O-ALY- <sup>5</sup> MeU	65.7	0.8	63.4	0.4	56.4	0.8
G	2'-O-PRG- <sup>5</sup> MeU	65.0	0.7	63.2	0.4	53.7	0.5
H	2'-O-BOE- <sup>5</sup> MeU	64.2	0.5	64.5	0.7	56.6	0.8
I	2'-O-DMAOE- <sup>5</sup> MeU	66.9	1.1	62.9	1.5		
J	2'-O-MAOE- <sup>5</sup> MeU	66.3	1.0				
K	2'-O-IME- <sup>5</sup> MeU	67.9	1.4	66.3	1.1	53.6	1.3

<sup>a</sup> L: 5' T\*CC AGG T\*GT\* CCG CAT\* C 3'. <sup>b</sup> M: 5' GCG T\*T\*T\*T\* T\*T\*T\*T\* T\*T\*T\*T\* T\*GC G 3'. <sup>c</sup> N: 5' CTC GTA CT\*T\*T\* T\*T\*T\*C CGG TCC 3'. <sup>d</sup> T<sub>m</sub> values were assessed buffer containing 100 mM Na<sup>+</sup>, 10 mM phosphate, 0.1 mM EDTA, pH 7, at 260 nm, and 4 μM oligonucleotides and 4 μM complementary length-matched RNA. Standard deviations do not exceed ±0.5 °C.

Following the general synthetic procedure for phosphoramidite synthesis (vide supra), nucleoside **11** (8.0 g, 12.97 mmol) was converted to **19** (9.11 g, 86% yield). <sup>31</sup>P NMR (80 MHz, CDCl<sub>3</sub>): δ 151.72, 151.18.

2'-O-(2-Fluoroethyl)-5'-O-(4,4'-dimethoxytrityl)-5-methyluridine-3'-[(2-cyanoethyl)-N,N-diisopropyl]phosphoramidite (**20**). Following the general synthetic procedure for phosphoramidite synthesis (vide supra), nucleoside **12** (3.0 g, 4.95 mmol) was converted to **20** (3.0 g, 78% yield). <sup>31</sup>P NMR (80 MHz, CDCl<sub>3</sub>): δ 151.26, 151.01.

2'-O-Trifluoroethyl-5'-O-(4,4'-dimethoxytrityl)-5-methyluridine-3'-[(2-cyanoethyl)-N,N-diisopropyl]phosphoramidite (**21**). Nucleoside **13** (10.00 g, 15.56 mmol) was converted to compound **21** (9.48 g, 71% yield) using the general synthetic procedure for phosphoramidites (vide supra). <sup>31</sup>P NMR (80 MHz, CDCl<sub>3</sub>): δ 151.76, 151.05.

2'-O-Allyl-5'-O-(4,4'-dimethoxytrityl)-5-methyluridine-3'-[(2-cyanoethyl)-N,N-diisopropyl]phosphoramidite (**22**). Following the general synthetic method for phosphoramidite synthesis (vide supra), compound **22** (3.2 g, 80% yield) was synthesized from **14** (3 g, 4.99 mmol).

2'-O-Propargyl-5'-O-(4,4'-dimethoxytrityl)-5-methyluridine-3'-[(2-cyanoethyl)-N,N-diisopropyl]phosphoramidite (**23**). Following the general method, compound **15** (4 g, 6.68 mmol) was converted into compound **23** (2.8 g, 53%). <sup>31</sup>P NMR (80 MHz, CDCl<sub>3</sub>): δ 151.82, 151.47.

2'-O-Benzoyloxyethyl-5'-O-(4,4'-dimethoxytrityl)-5-methyluridine-3'-[(2-cyanoethyl)-N,N-diisopropyl]phosphoramidite (**24**). Following the general method, compound **16** (3.3 g, 4.75 mmol) was converted into compound **24** (4.24 g, 92%). <sup>31</sup>P NMR (80 MHz, CDCl<sub>3</sub>): δ 150.85, 150.60.

5'-O-(4,4'-Dimethoxytrityl)-2'-O-(2-(imidazol-1-yl)-ethyl)-5-methyluridine-3'-[(2-cyanoethyl)-N,N-diisopropyl]phosphoramidite (**25**). Following the general method, compound **17** (2.2 g, 3.36 mmol) was converted into compound **25** (1.72 g, 60%). <sup>31</sup>P NMR (80 MHz, CDCl<sub>3</sub>): δ 151.52, 151.23.

**Oligonucleotide Synthesis, Purification, and Characterization.** All oligonucleotides were synthesized on functionalized controlled pore glass (CPG) on an automated solid phase DNA synthesizer using 0.1 M solution of the modified amidite **18–25** in anhydrous acetonitrile. The solid support functionalized with modified nucleosides **10–17** was used for the synthesis of oligonucleotides with 3'-modified

residues. For incorporation of A, G, C, and T residues standard phosphoramidites with exocyclic amino groups protected with benzoyl group (for A and C) and isobutyryl group (for G) were used. For incorporation of modified residues, phosphoramidite solutions were delivered in two portions, each followed by a 5 min coupling wait time. Oxidation of the internucleotide phosphite to phosphate was carried out using a 10% *tert*-BuOOH:acetonitrile:H<sub>2</sub>O (10:87:3) with 10 min waiting time or I<sub>2</sub>/pyridine/water. All other steps in the protocol supplied by the manufacturer were used without modification. The coupling efficiencies were >97%. After completion of the synthesis, the solid supports were suspended in aqueous ammonia (28–30 wt %, 2 mL for 2 μmol) at room temperature for 2 h to cleave the oligonucleotide from the solid support. The solid support was filtered off; the filtrate was then heated at 55 °C for 6 h to effect the complete removal of the base-labile protecting groups. Crude oligonucleotides were purified by high performance liquid chromatography (HPLC, C-4, Waters, 7.8 × 300 mm, A = 50 mM triethylammonium acetate (TEAAc), pH = 7, B = acetonitrile, 5% to 60% B in 55 min, flow 2.5 mL min<sup>-1</sup>, λ = 260 nm). The fractions containing full-length oligonucleotides were pooled together, and the pH of the solution was adjusted to 3.8 with acetic acid and the solution kept at room temperature until detritylation was complete (monitored by HPLC analysis). The detritylated oligonucleotides were desalted by HPLC on a Waters C-4 column to yield the 2'-modified oligonucleotides. Oligonucleotides were characterized by ESMS (see Table S1 of the Supporting Information), and purities were assessed by HPLC and capillary gel electrophoresis (CGE).

**Determination of RNA Affinity.** Absorbance versus temperature curves were measured at 260 nm using a Gilford Response II spectrophotometer interfaced to a PC. The buffer contained 100 mM Na<sup>+</sup>, 10 mM phosphate, 0.1 mM EDTA, pH 7. Oligonucleotide concentration was 4 μM; the concentration of each strand was determined from the absorbance at 85 °C, and extinction coefficients were calculated according to Puglisi and Tinoco (18). Each T<sub>m</sub> reported is the average of two experiments (Table 1). The ΔT<sub>m</sub> per modification was calculated by subtracting the T<sub>m</sub> of the unmodified DNA-RNA parent duplex from that of the duplex

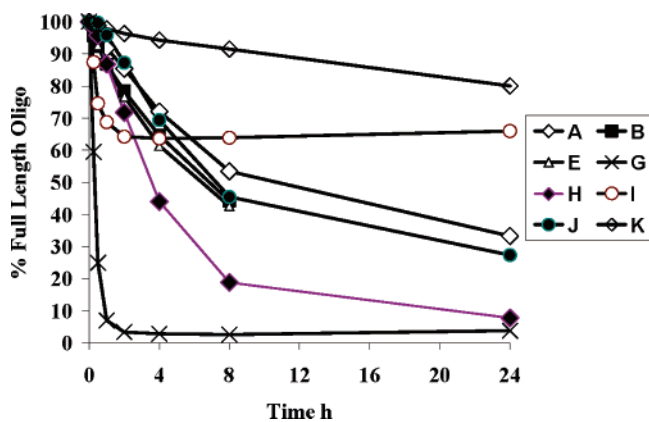


FIGURE 3: Relative nuclease resistance of the oligonucleotides with 2'-O-modifications A–K. A: T\* = 2'-O-MOE-<sup>5</sup>MeU. B: T\* = 2'-O-PRL-<sup>5</sup>MeU. E: T\* = 2'-O-TFE-<sup>5</sup>MeU. G: T\* = 2'-O-PRG-<sup>5</sup>MeU. H: T\* = 2'-O-BOE-<sup>5</sup>MeU. I: T\* = 2'-O-DMAOE-<sup>5</sup>MeU. J: T\* = 2'-O-MAOE-<sup>5</sup>MeU. K: T\* = 2'-O-IME-<sup>5</sup>MeU. The modifications were placed at the 3'-end of the sequence O, TTT TTT TTT TTT TTT T\* T\* T\* T\* T\*, and digested with snake venom phosphodiesterase. 5'-<sup>32</sup>P labeled oligonucleotides were digested with SVPD ( $5 \times 10^{-3}$  units mL<sup>-1</sup>) in 50 mM Tris-HCl buffer at pH 8.5, containing 72 mM NaCl and 14 mM MgCl<sub>2</sub> at 37 °C.

between RNA and modified strand and dividing by the number of modified residues in the sequence.

**Nuclease Stability Analysis.** The nuclease stability of the 2'-O-modified oligonucleotides was evaluated using snake venom phosphodiesterase as described previously (Figure 3 and Table S2, Supporting Information) (19).

**Crystallization and Data Collection and Processing.** The stock solutions of all chemically modified decamers of sequence 5'-d(GCGTAT\*ACGC) (T\* is the 2'-O-modified residue) were adjusted to concentrations of between 1 and 2 mM. Crystallizations were performed in hanging drops using the vapor diffusion technique. The commercially available Nucleic Acid Mini Screen (20) (Hampton Research, Aliso Viejo, CA) was used to establish crystallization conditions. Droplets containing oligonucleotide and buffer in 1:1 and 1:2 ratios were equilibrated against 0.5 mL of 35% (v/v) MPD. For seven of the modified decamers crystals obtained directly from the initial screen were used for structural analyses. In many cases several of the screened conditions resulted in crystals but only those that turned out to diffract to high resolution were used for further analysis. Crystals of the TFE decamer were grown using condition 5 (droplet composition: 10% MPD; 40 mM sodium cacodylate pH 6.0; 12 mM spermine tetra-HCl; 80 mM potassium chloride; 20 mM magnesium chloride). Crystals of the ALY, PRG, and PRL decamers were grown using condition 6 (10% MPD; 40 mM sodium cacodylate pH 6.0; 12 mM spermine tetra-HCl, 80 mM potassium chloride). The DMAOE and IME decamers were crystallized from conditions 8 (10% MPD; 40 mM sodium cacodylate pH 6.0; 12 mM spermine tetra-HCl; 80 mM sodium chloride) and 9 (10% MPD; 40 mM sodium cacodylate pH 6.0; 12 mM spermine tetra-HCl; 80 mM sodium chloride; 12 mM potassium chloride; 20 mM magnesium chloride), respectively. The BOE and FET decamers were crystallized from conditions 13 (10% MPD; 40 mM sodium cacodylate pH 6.0; 12 mM spermine tetra-HCl; 80 mM strontium chloride) and 17 (10% MPD; 40 mM sodium cacodylate pH 7.0; 12 mM spermine tetra-HCl; 80 mM sodium chloride), respectively. Improved crystals of the

FET decamer that were subsequently used for structure determination were obtained from droplets containing 1 mM oligonucleotide, 20 mM sodium cacodylate pH 6.0, 3 mM spermine tetra-HCl, and 10 mM calcium chloride. Crystals for the MAOE decamer were obtained from droplets containing 1 mM oligonucleotide, 20 mM sodium cacodylate pH 6.3, 2 mM spermine tetra-HCl, and 5 mM barium chloride. Crystals for the BTL decamer grew in the presence of 20 mM sodium cacodylate pH 6.3, 25% PEG 400, and either 150 mM magnesium or strontium chloride. Unlike the crystals of the other decamers containing 2'-O-modified residues that are all orthorhombic, BTL crystals exhibit tetragonal symmetry (Table 2).

For data collection, crystals were mounted in nylon loops and frozen in liquid nitrogen. All diffraction experiments except those with BTL crystals were carried out in-house on a Rigaku R-Axis IIC image plate system, mounted on a rotating anode X-ray generator. Various detector crystal distances, oscillation angles, and exposure times were used, but in general low- and high-resolution data were collected separately. Data for crystals of the BTL-modified decamer were collected on the 5-ID beam line of the Dupont-Northwestern-Dow Collaborative Access Team at the Advanced Photon Source (Argonne, IL). All data were integrated and merged with the DENZO and SCALEPACK programs, respectively (21), and selected data statistics are listed in Table 2.

**Structure Determination and Refinement.** The structures of all decamers are isomorphous to those with single 2'-O-modified thymidines studied earlier (13). The coordinates of the 2'-O-MOE-modified A-form DNA duplex structure minus the 2'-O-substituents and solvent molecules served as an initial model for rigid body refinement at medium resolution using the program CNS (22), followed by simulated annealing and inclusion of reflection data to full resolution. In all cases, 10% randomly chosen reflections were set aside for calculating *R*-free (23). Numerous rounds of positional and individual *B*-factor refinement cycles were then carried out, followed by addition of water molecules and metal ions and spermine molecules in structures where the latter were present. Sum ( $2F_o - F_c$ ) and difference ( $F_o - F_c$ ) Fourier electron density maps were displayed with the program TURBO FRODO (24) and revealed the two 2'-O-substituents per decamer duplex in all structures. Subsequently, CNS dictionary files were updated and refinement was continued until convergence of the *R*-work and *R*-free parameters was reached. The structure of the 2'-O-BTL-modified decamer duplex was determined by molecular replacement [AMoRe (25)] and refined with the program REFMAC (26). A summary of selected refinement parameters is given in Table 2.

## RESULTS AND DISCUSSION

**Synthesis of 2'-O-Modified Nucleosides and Oligonucleotides.** We have designed and synthesized several novel 2'-O-modified oligonucleotides (see Figure 2 for the structures and abbreviated names of the individual modifications). The modifications were designed to evaluate the effect of substituents at the 2'-position with varying chemistries and conformations on thermal stability as well as nuclease stability of oligonucleotides. The crystal structures of these

Table 2: Selected Crystal Data and Data Collection and Refinement Parameters

decamer	PRL	BTL <sup>a</sup>	FET	TFE	ALY	PRG	BOE	DMAOE	MAOE	IME
Crystal Data										
unit cell constants (Å)										
<i>a</i> (Å)	24.83	44.44	25.26	24.64	24.70	24.83	25.06	24.84	24.99	24.10
<i>b</i> (Å)	45.31	44.44	44.18	45.13	45.07	44.98	44.37	44.64	44.57	43.07
<i>c</i> (Å)	45.68	69.53	45.39	45.02	45.64	45.41	45.46	45.18	45.12	46.26
space group	<i>P</i> <sub>2</sub> <i>1</i> <sub>2</sub> <i>1</i>	<i>P</i> <sub>4</sub> <i>1</i> <sub>2</sub> <i>1</i>	<i>P</i> <sub>2</sub> <i>1</i> <sub>2</sub> <i>1</i>							
Data Collection										
resolution (Å)	1.50	2.30	1.70	1.50	1.60	1.55	1.80	1.65	1.60	1.60
no. of unique reflections	8698	3237	5893	7868	6760	7408	5065	6146	6913	6710
completeness (%)	99.4	100.0	98.3	91.8	94.1	94.9	98.7	95.4	97.5	99.2
<i>R</i> -merge, overall	0.053	0.075	0.074	0.070	0.071	0.062	0.074	0.102	0.068	0.096
last shell	0.407	0.390	0.281	0.261	0.222	0.265	0.348	0.175	0.337	0.376
Refinement										
reflections (no $\sigma$ cut)	8451	3223	5758	7593	6528	7257	4851	6099	6678	6507
completeness (%)	97.1	99.6	96.8	89.4	91.5	93.0	96.6	94.9	94.7	96.5
<i>R</i> -factor (%)	17.9	23.7	17.1	17.1	15.8	16.3	17.0	16.3	16.8	16.5
<i>R</i> -free (%)	21.6	26.0	18.9	20.2	18.5	20.5	21.3	19.1	20.0	18.9
no. of water molecules	128	31	103	115	131	125	101	124	106	114
ions (spm = spermine)		Mg <sup>2+</sup>		Mg <sup>2+</sup> /spm			Sr <sup>2+</sup>	2 Co <sup>3+</sup> /spm	Ba <sup>2+</sup>	3 Mg <sup>2+</sup> /spm
rms bond length (Å)	0.009	0.016	0.009	0.009	0.009	0.009	0.008	0.008	0.010	0.008
rms bond angles (deg)	1.30	1.82	1.41	1.31	1.32	1.29	1.28	1.20	1.44	1.37

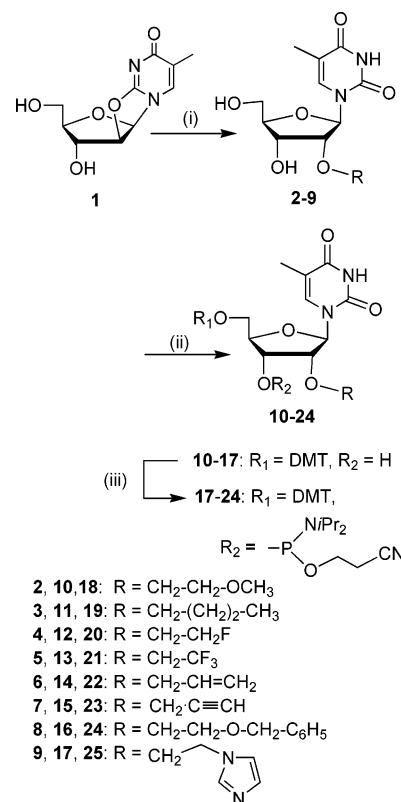
<sup>a</sup> The structure of a Sr<sup>2+</sup> form of the BTL-modified decamer was also determined: space group *P*<sub>4</sub>*1*<sub>2</sub>*1*, cell constants *a* = 43.57 Å, *c* = 69.94 Å, resolution 2.5 Å, *R*-factor 21.8%, *R*-free = 24.4%, 5 Sr<sup>2+</sup> ions per asymmetric unit, rms bonds/angles = 0.017 Å/1.68°.

modified oligonucleotides were also solved to probe the effect of the modifications on helical conformation and hydration of the modified oligonucleotides.

The oligonucleotides with 2'-*O*-DMAOE (Figure 2) and 2'-*O*-MAOE were synthesized as reported (27). Phosphoramidites **18–25** (Scheme 1) were used to synthesize oligonucleotides with 2'-*O*-modifications B–H and K (Figure 2). The syntheses of phosphoramidites **18–25** were accomplished as described in Scheme 1. The 2,2'-anhydro-5-methyluridine **1** heated with trialkyl borate esters of the corresponding alcohols at 150–160 °C gave the 2'-*O*-functionalized nucleosides **2–9**. The nucleosides were then treated with 4,4'-dimethoxytrityl chloride (DMTCl) in pyridine at room temperature to yield compounds **10–17**. Phosphitylation of **10–17** at the 3'-position afforded the phosphoramidite building blocks **18–25** in 60–78% yield. The nucleosides **10–17** were converted into 3'-*O*-succinyl derivatives and loaded onto the aminoalkyl controlled pore glass (CPG) to yield the functionalized CPG (40–50 μmol/g).

The 2'-*O*-modified oligonucleotides used in this study were synthesized on a solid phase DNA synthesizer. A 0.1 M solution of phosphoramidite in anhydrous acetonitrile was used for the synthesis. The overall coupling efficiency of modified phosphoramidite was >97%. All the oligonucleotides were characterized by ESMS, and purities were assessed by HPLC and capillary gel electrophoresis.

**Influence of 2'-*O*-Modifications on RNA Affinity.** The binding affinity of 2'-*O*-modified oligonucleotides to the target RNA was determined by obtaining the *T*<sub>m</sub> values from the temperature-dependent UV absorbance profile of the duplexes. The increases in *T*<sub>m</sub> of the 2'-*O*-modified oligonucleotides to complementary RNA range from 0.4 to 1.5 °C when modifications are placed in a row as in oligonucleotide M (Table 1) relative to the control DNA. When the modifications were placed in a dispersed design through the sequence as in L and N, the increases of *T*<sub>m</sub> vary between 0.5 and 1.4 °C. The gauche effect has been used to explain

Scheme 1<sup>a</sup>

<sup>a</sup> (i) BH<sub>3</sub>·THF, 150 °C. For **2**: 2-methoxyethanol. For **3**: *n*-butanol. For **4**: 2-fluoroethanol. For **5**: trifluoroethanol. For **6**: allyl alcohol. For **7**: propargyl alcohol. For **8**: 2-(phenylmethoxy)ethanol. For **9**: 1*H*-imidazole-4-ethanol. (ii) DMTCl, Py, DMAP, rt. (iii) 2-Cyanoethyl *N,N,N',N'*-tetraisopropylphosphorodiamidite, CH<sub>3</sub>CN, *N,N*-diisopropylaminetetrazolide, rt.

the high binding affinity of the 2'-*O*-MOE group (A, Table 1) (12, 13, 19). It is interesting to note that modifications with the possibility of extended gauche effects such as in 2'-*O*-MOE (Figure 2: D, 2'-*O*-FET; E, 2'-*O*-TFE; I, 2'-*O*-DMAOE; J, 2'-*O*-MAOE; and K, 2'-*O*-IME) exhibited higher

$T_m$  enhancement (Table 1, 0.9 to 1.4 °C per modification) compared to 2'-*O*-butyl-modified oligonucleotides (Table 1, C). All these modifications (A, D, E, H, J, K) should have a steric influence similar to that of 2'-*O*-butyl modification. The greater  $T_m$  enhancement exhibited by oligonucleotides modified with these modifications may suggest the role of stereoelectronic effects of the side chain on sugar pucker. 2'-*O*-Modifications such as 2'-*O*-propyl, 2'-*O*-allyl, 2'-*O*-propargyl, and 2'-*O*-butyl (B, F, G, and C) do not have a heteroatom to cooperate with the 2'-oxygen and thus extend the gauche effect from the furanose ring. Therefore, these modifications exhibited lesser degrees of  $T_m$  enhancement (0.4 to 0.8 °C per modification, Table 1). The exception is constituted by 2'-*O*-BOE (H, Table 1), which despite an oxygen atom in the side chain did not show an enhancement in  $T_m$  similar to that shown by modifications A, D, E, I, J, and K. The  $T_m$  enhancement (0.5 to 0.8 °C per modification) observed with 2'-*O*-BOE is similar to those of 2'-*O*-alkyl substituents. However, it is surprising that substitution at the 2'-position did not have an adverse effect on binding affinity, considering that bulky 2'-*O*-substituents could cause steric hindrance in the RNA-antisense oligomer duplex formed.

**Exonuclease Stability.** The exonuclease stability of the 2'-modified oligonucleotide O was evaluated using the snake venom phosphodiesterase (SVPD) assay (19) (Figure 3). The modifications in O were placed at the 3'-end, and all internucleosidic linkages were phosphodiester. The products of digestion at different time intervals were analyzed by PAGE and quantified using a phosphorimager. Figure 3 shows the comparative nuclease resistance of these modified oligonucleotides. A strong correlation between the stability of modified oligonucleotides and the nature of the modification was observed. Oligonucleotides with 2'-*O*-IME and 2'-*O*-DMAOE modifications exhibited exceptional stability ( $t_{1/2} > 24$  h, Table S2) whereas the 2'-*O*-PRG-modified oligonucleotide was the least stable ( $t_{1/2}$  0.3, Table S2). The  $t_{1/2}$  of the oligonucleotides with 2'-*O*-PRL (6.5 h), 2'-*O*-TFE (6 h), and 2'-*O*-MAOE (7.6 h) modifications were comparable. Oligonucleotides with 2'-*O*-BOE modification were degraded much more rapidly ( $t_{1/2}$  3.5 h, Table S2). The order of nuclease stability of modifications was 2'-*O*-IME > 2'-*O*-DMAOE > 2'-*O*-MOE > 2'-*O*-MAOE > 2'-*O*-PRL > 2'-*O*-TFE > 2'-*O*-BOE > 2'-*O*-PRG.

The superior stability of the zwitterionic 2'-*O*-IME and 2'-*O*-DMAOE modifications is in line with the high resistance to degradation by the positively charged 2'-*O*-aminopropyl (2'-*O*-AP) modification (14) as well as the 2'-*O*-{2-[2-(*N,N*-dimethylamino)ethoxy]ethyl} (DMAEOE, a fusion of the 2'-*O*-AP and 2'-*O*-MOE modifications (16)) and 2'-*O*-[2-(guanidinium)ethyl] [2'-*O*-GE (28)] modifications. Crystallographic data for complexes between DNA polymerase I Klenow fragment exonuclease and 2'-*O*-AP-modified oligodeoxynucleotides revealed that the additional protection afforded by positively charged sugar substituents is partly based on the ability of the positively charged moiety to displace a divalent metal ion required for exonuclease activity at the enzyme active site (15).

It is noteworthy that the 2'-*O*-BOE modification does not provide significant protection against nucleases and in fact is less effective than the relatively short 2'-*O*-alkyl substituents. These findings argue against the dogma that bulky

substituents commonly lead to higher nuclease resistance. Thus, the 2'-*O*-BOE modification represents an exception in terms of its effects on both RNA affinity and nuclease resistance; oligonucleotides containing 2'-*O*-BOE-modified residues exhibit higher RNA affinity than expected but yield only minor protection against exonuclease degradation considering the steric bulk.

**Crystal Structure Determination and Structure–Stability Correlations.** In order to gain insight into the conformational properties of the 2'-*O*-substituents and to potentially rationalize the observed differences in the thermal stability of duplexes between modified oligonucleotides and RNA as well as the different stabilities to nucleases exhibited by oligonucleotides carrying 2'-*O*-modified residues at their 3'-ends, we undertook detailed crystallographic studies. Decamers P [d(GCGTAT\*ACGC), T\* = 2'-*O*-modified-5-methyluridine] were synthesized and their crystal structures determined at high resolution. The self-complementary sequence d(GCGTATACGC) produces crystals of poor quality and low-resolution diffraction pattern that are consistent with adoption of a B-form DNA duplex (29). However, incorporation of single RNA or 2'-*O*-modified RNA residues at various locations produces crystals that diffract to high resolution, and the chimeric decamers then assume an A-form conformation (29–30). Thus a single ribonucleotide within an oligodeoxynucleotide can convert the duplex conformation from the B-form to the A-form (31). The conformational change may be aided by crystal packing forces and is most likely sequence-dependent. The above decamer sequence was selected as a template for investigating the structural properties of the 2'-*O*-substituents both because of the good resolution of the resulting crystal structures and because its geometry can be expected to resemble that of the duplex resulting from pairing between 2'-*O*-modified oligonucleotides and RNA.

Decamers d(GCGTAT\*ACGC) containing a single 2'-*O*-modified T\* nucleoside typically crystallize in an orthorhombic lattice with space group  $P2_12_12_1$  (Table 2). Therefore, the two duplex strands are not related by symmetry and each structure yields the conformation of two independent 2'-*O*-modified residues. The 2'-*O*-BTL-modified decamer constitutes an exception because crystals have tetragonal symmetry, rendering the two duplex strands identical. The numbering of residues in the duplexes is 1 to 10 for strand 1 and 11 to 20 for strand 2; the 2'-*O*-modified residues are T\*6 and T\*16. All structures were determined by molecular replacement and were refined with the program CNS (22) except for the BTL decamer, whose structure was refined with the program REFMAC (26). Selected crystal data, data collection, and refinement parameters for all 10 crystal structures are summarized in Table 2. Examples of the quality of the final electron density are depicted in Figure 4. In every structure except that of the BTL decamer, both 2'-*O*-substituents were completely visible in electron density maps. Only three of the four carbon atoms of the 2'-*O*-BTL substituent were observed, and the terminal methyl group appears to be disordered.

Atomic-resolution structures of the 2'-*O*-FET and 2'-*O*-AOE-modified decamer duplexes were previously deposited in the Protein Data Bank as part of an analysis of metal–cation interactions (32) [PDB ID codes: 1I0F (AOE decamer at 1.7 Å resolution; see following discussion), 1I0M (Rb<sup>+</sup>

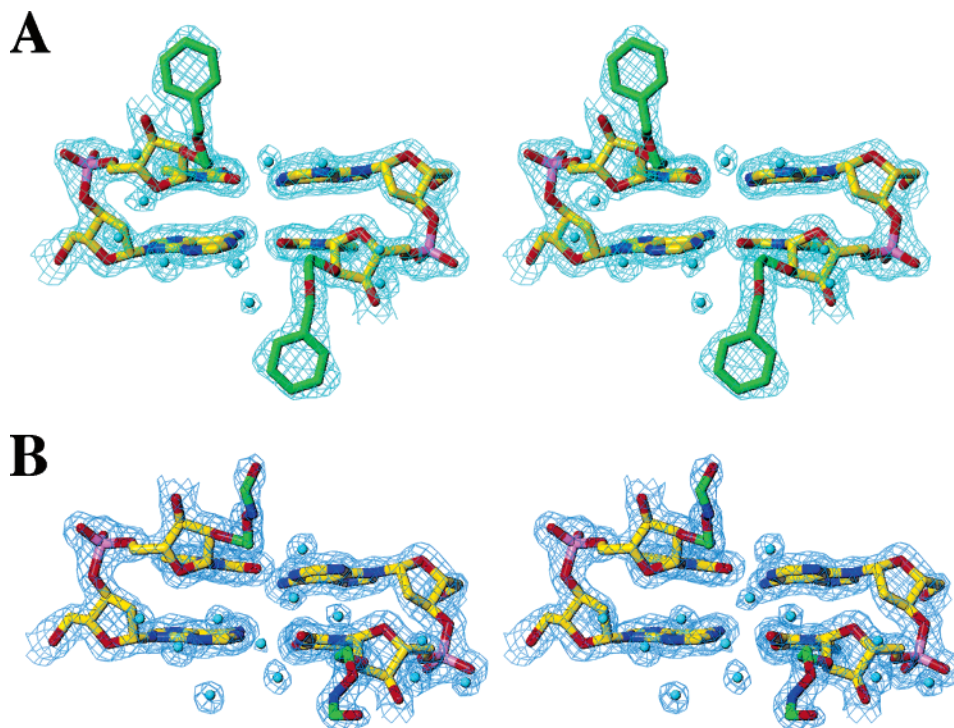


FIGURE 4: Final sum ( $2F_o - F_c$ ) Fourier electron densities ( $1\sigma$  level) around selected 2'-O-substituents: (A) BOE; (B) MAOE. Carbon atoms of substituents are highlighted in green, and water molecules are cyan spheres.

form of FET decamer at 1.05 Å), and 110G (Na<sup>+</sup>-form of FET decamer at 1.45 Å)]. However, the conformations of the 2'-O-substituents and their hydration were not explicitly discussed at the time. Unexpectedly, electron density maps for the decamer carrying 2'-O-MAOE moieties indicated longer chains for the substituents than anticipated. It was concluded that a portion of the assumed 2'-O-(2-aminoxy)-ethyl substituents (AOE: O2'-CH<sub>2</sub>-CH<sub>2</sub>-O-NH<sub>2</sub>; the above deposited structure) had reacted with formaldehyde to give the 2'-O-[2-[(methyleneamino)oxy]ethyl] compound (MAOE: O2'-CH<sub>2</sub>-CH<sub>2</sub>-O-N=CH<sub>2</sub>; Figure 2). This is further complicated by the observation (based on the local electron density; Figure 4B) that the dehydration step with some of the material appears not to have proceeded to completion, resulting in the formation of a substituent that is extended by a hydroxyl group relative to MAOE (O2'-CH<sub>2</sub>-CH<sub>2</sub>-O-NH-CH<sub>2</sub>-OH; Figure 5J). Thus, the electron density probably represents a composite of the AOE, MAOE, and hydroxy-MAOE substituents.

Stereodiagrams for each of the 2'-O-modified base pair steps (A5pT\*6):(A15pT\*16) in the decamer duplexes are depicted in Figure 5. Short 2'-O-substituents (PRL, BTL, FET, TFE, ALY, and PRG) project away from the duplex at the border of the minor groove, whereas the longer ones show a tendency to fold back on the duplex and associate with backbone or base atoms. A feature shared among all 20 2'-O-modified riboses is the antiperiplanar (*ap*) conformation of the C3'-C2'-O2'-CA' torsion angle (substituent atoms are labeled CA', CB', C/O/FC', etc.). This was first observed in the crystal structure of a 2'-O-methyl-modified duplex (33) and is also a staple of 2'-O-MOE-modified riboses (12, 13) (Figure 5a). Such a conformation prevents potentially unfavorable interactions between sugar and substituent as seen in the case of the crystal structure of a duplex containing 2'-O-ethoxymethylene (2'-O-EOM) moieties,

where the local backbone geometry was altered and stacking reduced as a result of an anticlinal (*ac*-) conformation of the C3'-C2'-O2'-CA' torsion in the EOM-modified thymidine (13). In all 2'-O-substituents with electronegative outer atoms (O, MOE, BOE, DMAOE, MAOE, IMI; and F, FET, TFE) or moieties (double bond, ALY) that are separated by an ethyl linker from O2', the torsion angles around the C-C bond adopt synclinal (*sc*+ or *sc*-) conformations. Thus, the conformational preorganization as a result of the gauche effect between O2' and electron-withdrawing atoms or moieties in the substituents is clearly borne out by the structural data.

Another recurring feature of 2'-O-modified residues in the structures of the decamers is a water molecule that is trapped between O2' and O3' and, where possible, engages in an additional interaction to the outer acceptor or donor atoms of some of the substituents (a C=C double bond in the case of ALY) (Figure 5). In 2'-O-MOE modified nucleosides, this mode of hydration was found throughout a fully modified MOE-RNA dodecamer duplex, with water molecules in hydrogen-bonding distance from OC', O2, and O3' (Figure 5A). Thanks to the availability of a diverse set of 2'-O-modified structures, it now appears that the basic motif involves only the 2'- and 3'-oxygen atoms from the ribose. Thus, the position of the water molecule is practically conserved also with 2'-O-PRL- and 2'-O-BTL-modified residues (Figures 5B,C). However, closer inspection of the water structure propagating from the water molecule coordinated to O2' and O3' indicates that acceptor or donor atoms, such as those present in the DMAOE (Figure 5I) or MAOE (Figure 5J) substituents, appear to promote a more extensive solvent network. In some cases, waters link 2'-O-substituent and 3'-phosphate group (12) (data not shown). Creation of a stable water structure beyond the hydration usually associated with the phosphate backbones or edges of nucleo-

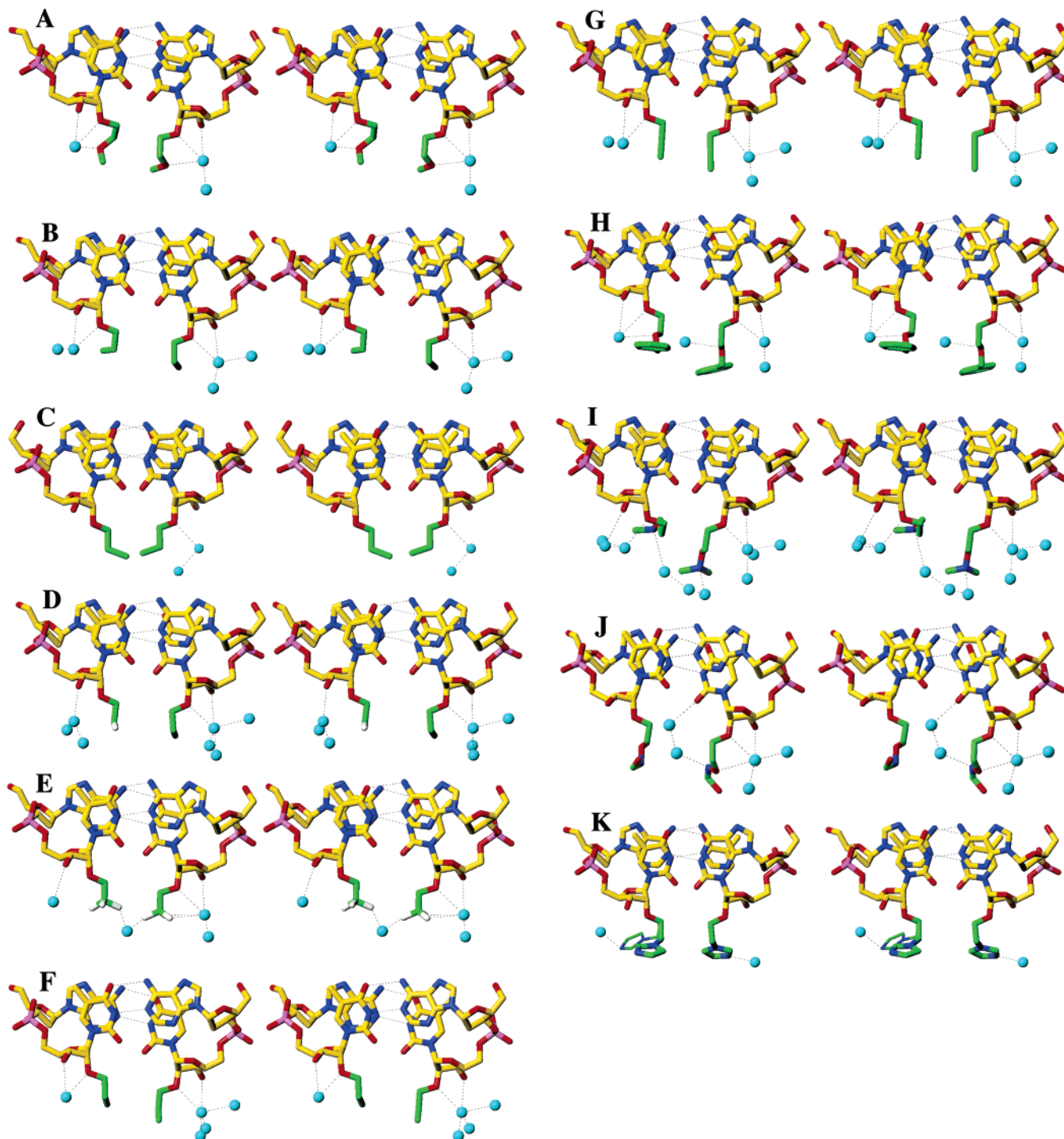


FIGURE 5: Stereodiagrams of the conformation and hydration of the 2'-*O*-modified base pair steps (A5pT\*6):A15pT\*16) in the 10 different decamer duplexes with sequence d(GCGTAT\*ACGC) and the reference 2'-*O*-MOE-modified structure (13). The views are roughly along the normal to the plane defined by the top base pair and thus correspond to the views depicted in Figure 4 rotated by 90° around the horizontal; residue 6 is on the left, and residue 16 is on the right: (A) MOE; (B) PRL; (C) BTL; (D) FET; (E) TFE; (F) ALY; (G) PRG; (H) BOE; (I) DMAOE; (J) MAOE; (K) IME. Carbon atoms of substituents are green, water molecules are cyan spheres, and hydrogen bonds are dashed lines.

bases in the grooves can be expected to account for at least a part of the increased gains in RNA affinity observed for the DMAOE and IME modifications compared to the more simple alkyl (PRL and BTL) and ALY substituents. For example, DMAOE substituents are oriented at the periphery of the minor groove in such a way that their *N,N*-(dimethyl)-ammonium moieties can be bridged by a trio of water molecules (Figure 5I). In addition, DMAOE substituents

engage in water-mediated contacts to base atoms in the minor groove (not shown).

In the structure of the decamer duplex with 2'-*O*-BOE modifications, both substituents are fully ordered and the observed similar conformations are consistent with the surprisingly high increase in  $T_m$  afforded by the 2'-*O*-BOE modification. Thus, the phenyl ring is located above the backbone and points toward the 3'-end of the strand (Figure

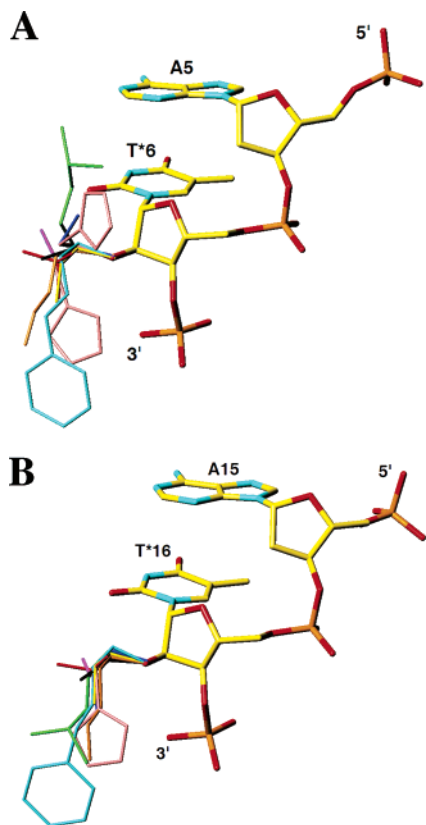


FIGURE 6: Superpositions of 2'-O-substituents of (A) residues T\*6 and (B) residues T\*16. Color code: blue (PRL), yellow (FET), red (TFE), pink (ALY), black (PRG), cyan (BOE), green (DMAOE), orange (MAOE), and beige (IME).

5H). The distances between the C5' and C4' atoms from the adjacent adenosine and the phenyl ring along the normal to the ring plane are about 3.9 Å (Figure 6). Thus, in oligonucleotides with consecutive 2'-O-BOE modifications (M and N, Table 1), one would not expect steric crowding of the minor groove by 2'-O-BOE substituents from residues located on opposite strands or unfavorable interactions between substituents from adjacent thymidines in the same strand. Hence, the somewhat surprising gains in RNA affinity observed for 2'-O-BOE-modified oligonucleotides.

Interestingly, in the majority of cases, the other longer 2'-O-substituents (DMAOE, MAOE, and IME) are also directed toward the 3'-termini of strands (Figures 5, 6). For residue T\*6 in the 2'-O-IME-modified duplex two orientations of the substituent were observed (Figures 5K, 6). In about half the molecules in the crystal, the substituent is pointing toward the 3'-terminus of the strand, and in the other half, it is directed toward the 5'-terminus. In the structure of the 2'-O-DMAOE-modified duplex, only one of the substituents snakes along the backbone, whereas the other is directed into the minor groove (Figures 5I, 6). The preference for the substituent's alignment relative to the direction of the strand may in part be due to lattice interactions. In the orthorhombic crystals, terminal base pairs of two different duplexes stack into the minor groove at opposite ends of a third duplex (29). Although the central portion of the minor groove is devoid of close contacts between adjacent duplexes, the outer atoms of longer 2'-O-substituents will get to lie in close proximity of the sugar-phosphate backbone from a symmetry-related duplex (Figure 7). An analysis of potential steric clashes between substituents and neighboring duplexes provides a

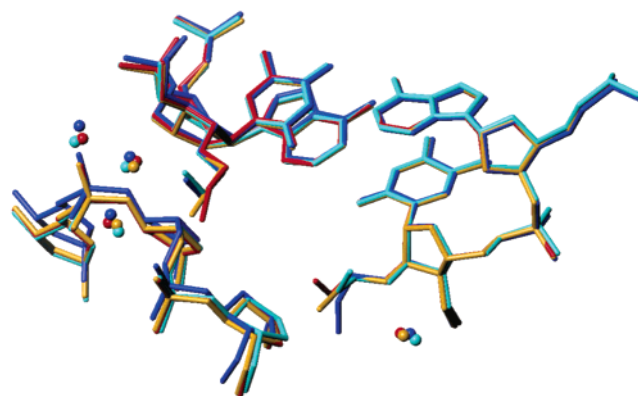


FIGURE 7: Packing interactions in the orthorhombic crystal lattice of 2'-O-modified DNA decamers. The observed preference of longer 2'-O-substituents to align themselves with the sugar-phosphate backbone such that they are directed toward the 3'-terminus may be influenced by packing (see left-hand side of diagram). A portion of the backbone from a neighboring duplex can be seen crossing the reference duplex (only the A5pT\*6:A15pT\*16 dimer is shown). A third duplex that associates with the strand of the reference duplex on the right in a similar fashion has been omitted for clarity. Orientations of longer 2'-O-substituents such that they would point toward the 5'-terminus of the modified strand may generate unfavorable interactions with symmetry mates. Color code: yellow (PRG), red (ALY), cyan (PRL), and blue (FET). Water molecules trapped between substituent and sugar are shown as spheres.

rationale for the preferred mode of alignment of BOE, DMAOE, MAOE, and IME substituents discussed above. The exceptions seen for one of the DMAOE and IME substituents are most likely due to the fact that both are carrying a positive charge. Potentially unfavorable interactions due to limited space between 2'-O-substituent and backbone atoms from a neighboring duplex may become attractive as a result of the positive charge on the substituent. A clear indication of the effects of charge is seen in the somewhat tighter stacking between the imidazolyl moiety of IME and the C4' and C5' backbone atoms from the adjacent residue below (ca. 3.6 Å) compared to the situation in the structure of the 2'-O-BOE-modified duplex (vide supra; Figure 6).

The higher nuclease resistances afforded by the IME and DMAOE modifications are most likely also a direct consequence of the positive charge. Both 2'-O-substituents engage in water-mediated interactions with the 3'-phosphate group. A stable solvent network combined with shielding of the phosphate group by the positively charged moiety of the substituent should provide protection against nuclease degradation. Apparently, this is much more effective than the addition of steric bulk to the backbone as evidenced by the surprisingly efficient degradation of an oligonucleotide modified with 2'-O-BOE-Ts at the 3'-end by an exonuclease (Figure 3). In the crystal structure, the phenyl moiety of 2'-O-BOE substituents is relatively far removed from the phosphate groups of adjacent intrastrand residues. By comparison, imidazolyl rings of 2'-O-IME substituents and phosphate groups are more closely spaced, with one of the rings for residue T\*6 practically sitting above the 3'-phosphate ( $N^+\cdots OP = 4.1$  Å). Judging from the crystallographic data, 2'-O-substituents such as PRL, FET, ALY, and particularly PRG are too short and too far removed from the phosphate group to significantly affect binding and processing by exonucleases.

## CONCLUSIONS

We have analyzed the RNA hybridization, nuclease resistance, and crystal structures of oligonucleotides containing a series of 2'-*O*-modifications. In all cases, modification increases the RNA affinity relative to DNA. The stability increases observed with longer and in some cases positively charged 2'-*O*-substituents slightly exceed those seen with shorter and highly electronegative 2'-*O*-substituents. Factors that account for the somewhat higher stability afforded by charged substituents are close proximity between the positive moiety and the 3'-phosphate group of the modified residue, and water-mediated interactions between substituent atoms and phosphates and/or base functionalities. Consecutively placed substituents in a strand can also be expected to stabilize a network of water molecules in the minor groove that is absent in native DNA or RNA. This view is supported by the observation in the structure that 2'-*O*-DMAOE substituents from opposite strands can be bridged by a chain of water molecules at the periphery of the minor groove.

Substituents carrying a positive charge such as DMAOE and IME or atoms in the outer region that can act as hydrogen bonding donors or acceptors (i.e. MAOE or MOE) also furnish better protection against nuclease degradation than the smaller aliphatic substituents (PRL) or those featuring electron-withdrawing atoms (FET, TFE) or moieties (ALY, PRG). The crystal structures demonstrate that the IME and DMAOE substituents can shield the neighboring phosphate group via water-mediated and "stacking" interactions (IME). The BOE substituent represents an exception both in terms of the unexpectedly high RNA affinity and low nuclease resistance observed with this modification. Structural data are consistent with a well-ordered benzyl moiety that stacks against the C4'-C5' bond of the residue 3'-adjacent to the 2'-*O*-modified thymidine. Conformational preorganization and electrostatic interactions with backbone atoms can account for the favorable hybridization properties exhibited by 2'-*O*-BOE-modified oligonucleotides. The low resistance to exonucleases of 2'-*O*-BOE-modified oligonucleotides goes against the assumption that steric bulk will necessarily lead to better protection. In the crystal structure, the benzyl moiety is not in the close vicinity of the phosphate group. Conversely, the highly protective IME modification is closely associated with the adjacent phosphate group, providing electrostatic and steric obstacles for the exonuclease and potentially interfering with metal-ion binding at the active site of the enzyme (15).

Although the 2'-*O*-modifications analyzed here were originally designed for further in vivo pharmacokinetic and biodistribution evaluations in potential antisense therapeutics, we would like to emphasize that the favorable hybridization properties and nuclease resistances exhibited by some of them may warrant more detailed tests regarding their use in chemically modified small interfering RNAs (siRNAs). RNA interference (RNAi) experiments using chemically modified siRNAs have only been conducted to a limited extent, and relatively few modifications have been evaluated in vitro or in vivo to date (reviewed in ref 34). Given the fact that the 2'-fluoro (35) and, more recently, the 2'-*O*-methyl modification in combination with cholesterol conjugation in an in vivo application (36) have shown increased activity in silencing of genes via RNAi, 2'-*O*-modifications with

promising properties regarding RNA affinity and nuclease protection that we have analyzed here may well proceed to more detailed trials in the context of RNAi.

## SUPPORTING INFORMATION AVAILABLE

Mass spectral analysis of 2'-*O*-modified oligonucleotides (Table S1) and exonuclease stability of 2'-*O*-modified oligonucleotide phosphodiester (Table S2). This material is available free of charge via the Internet at <http://pubs.acs.org>.

## REFERENCES

- Freier, S. M., and Altmann, K. H. (1997) The ups and downs of nucleic acid duplex stability: structure-stability studies on chemically-modified DNA:RNA duplexes, *Nucleic Acids Res.* 25, 4429–4443.
- Crooke, S. T. (1998) Basic principles of antisense therapeutics, in *Antisense Research and Application* (Crooke, S. T., Ed.) Vol. 131, pp 1–50, Springer, Berlin.
- Crooke, S. T. (1995) Phosphorothioate oligonucleotides, in *Therapeutic Applications of Oligonucleotides* (Crooke, S. T., Ed.) pp 63–79, R. G. Landes, Austin.
- Manoharan, M. (1999) 2'-Carbohydrate modifications in antisense oligonucleotide therapy: importance of conformation, configuration and conjugation, *Biochim. Biophys. Acta* 1489, 117–130.
- Cummins, L. L., Owens, S. R., Risen, L. M., Lesnik, E. A., Freier, S. M., McGee, D., Guinosso, C. J., and Cook, P. D. (1995) Characterization of fully 2'-modified oligoribonucleotide hetero- and homoduplex hybridization and nuclease sensitivity, *Nucleic Acids Res.* 23, 2019–2024.
- Lesnik, E. A., Guinosso, C. J., Kawasaki, A. M., Sasmor, H., Zounes, M., Cummins, L. L., Ecker, D. J., Cook, P. D., and Freier, S. M. (1993) Oligodeoxynucleotides containing 2'-*O*-modified adenosine: synthesis and effects on stability of DNA:RNA duplexes, *Biochemistry* 32, 7832–7838.
- De Mesmaeker, A., Häner, R., Martin, P., and Moser, H. E. (1995) Antisense oligonucleotides, *Acc. Chem. Res.* 28, 366–374.
- Martin, P. (1995) New access to 2'-*O*-alkylated ribonucleosides and properties of 2'-*O*-alkylated oligoribonucleotides, *Helv. Chim. Acta* 78, 486–504.
- Altmann, K. H., Fabbro, D., Dean, N. M., Geiger, T., Monia, B. P., Muller, M., and Nicklin, P. (1996) Second-generation antisense oligonucleotides: structure-activity relationships and the design of improved signal-transduction inhibitors, *Biochem. Soc. Trans.* 24, 630–637.
- Altmann, K.-H., Dean, N. M., Fabbro, D., Freier, S. M., Geiger, T., Häner, R., Hüsken, D., Martin, P., Monia, B. P., Müller, M., Natt, F., Nicklin, P., Phillips, J., Pieleis, U., Sasmor, H., and Moser, H. E. (1996) Second generation of antisense oligonucleotides: from nuclease resistance to biological efficacy in animals, *Chimia* 50, 168–176.
- Khatsenko, O., Morgan, R., and Geary, R. (1998) Effect of oligonucleotide size and chemistry on intestinal absorption in an in situ rat model. *AAPS Pharm. Sci.* 1, No. 1. (website: [http://www.aapspharmsci.org/abstracts/am\\_abstracts2002.asp](http://www.aapspharmsci.org/abstracts/am_abstracts2002.asp))
- Teplova, M., Minasov, G., Tereshko, V., Inamati, G. B., Cook, P. D., Manoharan, M., and Egli, M. (1999) Crystal structure and improved antisense properties of 2'-*O*-(2-methoxyethyl)-RNA, *Nat. Struct. Biol.* 6, 535–539.
- Tereshko, V., Portmann, S., Tay, E. C., Martin, P., Natt, F., Altmann, K.-H., and Egli, M. (1998) Correlating structure and stability of DNA duplexes with incorporated 2'-*O*-modified RNA analogues, *Biochemistry* 37, 10626–10634.
- Griffey, R. H., Monia, B. P., Cummins, L. L., Freier, S., Greig, M. J., Guinosso, C. J., Lesnik, E., Manalili, S. M., Mohan, V., Owens, S., Ross, B. R., Sasmor, H., Wanczewicz, E., Weiler, K., Wheeler, P. D., and Cook, P. D. (1996) 2'-*O*-Aminopropyl ribonucleotides: a zwitterionic modification that enhances the exonuclease resistance and biological activity of antisense oligonucleotides, *J. Med. Chem.* 39, 5100–5109.
- Teplova, M., Wallace, S. T., Minasov, G., Tereshko, V., Symons, A., Cook, P. D., Manoharan, M., and Egli, M. (1999) Structural origins of the exonuclease resistance of a zwitterionic RNA, *Proc. Natl. Acad. Sci. U.S.A.* 96, 14240–14245.

16. Prhavc, M., Prakash, T. P., Minasov, G., Egli, M., and Manoharan, M. (2003) 2'-O-[2-[2-(*N,N*-Dimethylamino)ethoxy]ethyl] modified antisense oligonucleotides: symbiosis of charge interaction factors and stereoelectronic effects, *Org. Lett.* 5, 2017–2020.
17. Prakash, T. P., Manoharan, M., Fraser, A. S., Kawasaki, A. M., Lesnik, E., Sioufi, N., Leeds, J. M., Teplova, M., and Egli, M. (2002) 2'-O-[2-(Methylthio)ethyl]-modified oligonucleotide: an analog of 2'-O-[2-(methoxy)ethyl]-modified oligonucleotide with improved protein binding properties and high binding affinity to target RNA, *Biochemistry* 41, 11642–11648.
18. Puglisi, J. D., and Tinoco Jr., I. (1989) Absorbance melting curves of RNA, *Methods Enzymol.* 180, 304–325.
19. Cummins, L. L., Owens, S. R., Risen, L. M., Lesnik, E. A., Freier, S. M., McGee, D., Guinosso, C. J., and Cook, P. D. (1995) Characterization of fully 2'-modified oligoribonucleotide hetero and homoduplex hybridization and nuclease sensitivity, *Nucleic Acids Res.* 23, 2019–2024.
20. Berger, I. Kang, C. H., Sinha, N., Wolters, M., and Rich, A. (1996) A highly efficient 24-condition matrix for the crystallization of nucleic acid fragments, *Acta Crystallogr. D* 52, 465–468.
21. Otwinowski, Z., and Minor, W. (1997) Processing of X-ray diffraction data collected in oscillation mode, *Methods Enzymol.* 276, 307–326.
22. Brünger, A. T., Adams, P. D., Clore, G. M., DeLano, W. L., Gros, P., Grosse-Kunstleve, R. W., Jiang, J. S., Kuszewski, J., Nilges, M., Pannu, N. S., Read, R. J., Rice, L. M., Simonson, T., and Warren, G. L. (1998) Crystallography & NMR System: A new software suite for macromolecular structure determination, *Acta Crystallogr. D* 54, 905–921.
23. Brünger, A. T. (1992) Free R value: a novel statistical quantity for assessing the accuracy of crystal structures, *Nature* 355, 472–475.
24. Cambillau, C., and Roussel, A. (1997) Turbo Frodo, Version OpenGL.1, Université Aix-Marseille II, Marseille, France.
25. Navaza, J. (1997) AMoRe: An automated molecular replacement program package. *Methods Enzymol.* 276, 581–594.
26. Murshudov, G. N., Vagin, A. A., and Dodson, E. J. (1997) Refinement of macromolecular structures by the maximum-likelihood method, *Acta Crystallogr. D* 53, 240–255.
27. (a) Prakash, T. P., Kawasaki, A. M., Fraser, A. S., Vasquez, G., and Manoharan, M. (2002) Synthesis of 2'-O-[2-[(*N,N*-Dimethylamino)oxy]ethyl] Modified Nucleosides and Oligonucleotides, *J. Org. Chem.* 67, 357–369. (b) Kawasaki, A. M., Casper, D. M., Prakash, T. P., Manalili, S., Sasmor, H., Manoharan, M., and Cook, D. C. (1999) Synthesis, hybridization, and nuclease resistance properties of 2'-O-aminooxyethyl (2'-O-AOE) modified oligonucleotides, *Tetrahedron Lett.* 40, 661–664.
28. Prakash, T. P., Pueschl, A., Lesnik, E., Tereshko, V., Egli, M., and Manoharan, M. (2004) 2'-O-[2-(guanidinium)ethyl]-5-methyluridine modified oligonucleotides: synthesis and stabilizing effect on duplex and triplex nucleic acid structures, *Org. Lett.* 6, 1971–1974.
29. Egli, M., Usman, N., and Rich, A. (1993) Conformational influence of the ribose 2'-hydroxyl group: crystal structures of DNA-RNA chimeric duplexes, *Biochemistry* 32, 3221–3237.
30. Egli, M. (1998) Towards the structure-based design of nucleic acid therapeutics, in *Advances in Enzyme Regulation* (Weber, G., Ed.) Vol. 38, pp 181–203, Elsevier Science Ltd., Oxford, U.K.
31. Ban, C., Ramakrishnan, B., and Sundaralingam, M. (1994) A single 2'-hydroxyl group converts B-DNA to A-DNA. Crystal structure of the DNA-RNA chimeric decamer d(CCGGC)r(G)d(CCGG) with a novel intermolecular G•C base-paired quadruplet, *J. Mol. Biol.* 236, 275–285.
32. Tereshko, V., Wilds, C. J., Minasov, G., Prakash, T. P., Maier, M. A., Howard, A., Wawrzak, Z., Manoharan, M., and Egli, M. (2001) Detection of alkali metal ions in DNA crystals using state-of-the-art X-ray diffraction experiments, *Nucleic Acids Res.* 29, 1208–1215.
33. Lubini, P., Zürcher W., and Egli, M. (1994) Crystal structure of an oligodeoxynucleotide duplex containing 2'-O-methylated adenosines, *Chem. Biol.* 1, 39–45.
34. Manoharan, M. (2004) RNA interference and chemically modified small interfering RNAs, *Curr. Opin. Chem. Biol.* 8, 570–579.
35. Allerson, C. R., Sioufi, N., Jarres, R., Prakash, T. P., Naik, N., Berdeja, A., Wanders, L., Griffey, R. H., Swayze, E. E., and Bhat, B. (2005) Fully 2'-modified oligonucleotide duplexes with improved in vitro potency and stability compared to unmodified siRNA, *J. Med. Chem.* 48, 901–904.
36. Soutschek, J., Akinc, A., Bramlage, B., Charisse, K. Constien, R., Donoghue, M., Elbashir, S., Geick, A., Hadwiger, P., Harborth, J., John, M., Kesavan, V., Lavine, G., Pandey, R. K., Racie, T., Rajeev, K. G., Röhl, I., Toudjarska, I., Wang, G., Wuschko, S., Bumcrot, D., Kotliansky, V., Limmer, S., Manoharan, M., and Vornlocher, H.-P. (2004) Therapeutic silencing of an endogenous gene by systemic administration of modified siRNAs, *Nature* 432, 173–178.

BI050574M